ISSN 1062-8738, Bulletin of the Russian Academy of Sciences: Physics, 2021, Vol. 85, No. 4, pp. 464–467. © Allerton Press, Inc., 2021.
Russian Text © The Author(s), 2021, published in Izvestiya Rossiiskoi Akademii Nauk, Seriya Fizicheskaya, 2021, Vol. 85, No. 4, pp. 605–608.

Study of Forbush Effects during Powerful Solar Flares by the URAGAN Muon Hodoscope Data

A. A. Kovylyaeva[a, b, *], N. S. Barbashina[a], V. G. Getmanov[b, c], A. N. Dmitrieva[a, b], M. N. Dobrovolsky[b], Yu. N. Mishutina[a], A. A. Soloviev[b, c], V. E. Chinkin[b], V. V. Shutenko[a], E. I. Yakovleva[a], and I. I. Yashin[a, b]

[a] *National Research Nuclear University (MEPhI), Moscow, 115409 Russia*
[b] *Geophysical Center, Russian Academy of Sciences, Moscow, 119296 Russia*
[c] *Schmidt Institute of Physics of the Earth, Russian Academy of Sciences, Moscow, 123995 Russia*
**e-mail: AAKovylyaeva@mephi.ru*

Received October 19, 2020; revised November 19, 2020; accepted November 27, 2020

Abstract—Forbush effects caused by powerful X-class solar flares are studied using URAGAN muon hodoscope data for the period 2007–2019. The URAGAN muon hodoscope registers the cosmic ray muon flux on the Earth's surface from different directions simultaneously. This allows study of the energy, angular, and space–time characteristics of variations in the cosmic ray muon flux during Forbush effects. The dependence of the measured Forbush effects on the parameters of heliospheric and geomagnetic disturbances is analyzed.

DOI: 10.3103/S1062873821030126

INTRODUCTION

Solar flares are the most intense disturbances of space weather. High-energy protons and electrons are ejected during a solar flare, along with intense radiation at all wavelengths that can affect not only the upper layers of the Earth's atmosphere but the propagation of radio waves as well. The higher level of X-ray and extreme ultraviolet radiation ionizes the ionosphere on the sunlit side of the Earth. The intense X-ray radiation causes absorption in the lower layer of the ionosphere, which results in the deterioration or full absorption (i.e., radio signal cutoff) of high-frequency signals. Solar flares are classified according to their peak radiation in the spectral range of 0.1–0.8 nm (i.e., in the X-ray range). They are denoted by letters A, B, C, M, and X, X-class flares being the ones most intense with emissions above 10^{-4} W m^{-2} [1].

The Forbush effect (FE) in geophysics is a rapid decrease in the intensity of cosmic rays (CRs), due to the diversion of charged particles by inhomogeneities in the interplanetary magnetic field. This decrease in CR intensity is caused by the diversion of primary cosmic radiation particles by different large-scale inhomogeneities: the magnetic fields of solar plasma clouds that form during coronal mass ejections (CMEs); shock waves created during the motion of high-speed solar wind fluxes rotating together with the Sun and originating from coronal holes; and other phenomena in the heliosphere. The FE can also be observed not only on the Earth but on space vehicles as well. The physicist Scott Forbush noticed that the intensity of cosmic rays reaching the Earth did not correlate with the number of sunspots during the 11-year cycle of solar activity, since there were more cosmic rays at the minimum of the cycle and fewer at the maximum [2]. At the maximum of solar activity, stronger magnetic fields are carried out into interplanetary space by the solar wind, and these fields block cosmic rays.

Fluxes of cosmic rays are now detected primarily by the worldwide network of neutron monitors [3] and muon telescopes [4]. The large-area URAGAN muon hodoscope (MH) operates on the territory of National Research Nuclear University (MEPhI) [5]. A distinctive feature of the URAGAN muon hodoscope compared to other ground-based facilities is the possibility of reconstructing the trajectory of each muon from all directions of the upper hemisphere.

In this work, we study FEs detected in the muon cosmic ray flux according to MH URAGAN data. Thirteen FEs caused by X-class flares were selected from among 103 events with FE amplitudes $A_{\rm FD}$ > 0.5% in the period 2007–2019. We analyzed the relation between the obtained characteristics of Forbush effects and the parameters of heliospheric and geomagnetic disturbances. The events of March 8, 2012, and September 8, 2017, caused by X-class flares and accompanied by the largest decrease in the *Dst* index were considered in detail.

Table 1. Forbush effects caused by powerful X-class solar flares, according to muon hodoscope URAGAN data for the period 2007–2019

No.	Flare beginning, UT	Start of FE, UT	Δt, days	A_{FD}, %	V_{SW}, km/s	B, nT	Dst_{min}, nT	Flare class	Coordinates
1	Feb. 15, 2011 01:44	Feb. 18, 2011 02:30	3.0	1.3 ± 0.1	691	30.6	−27	X2.2	S20W12
2	Sept. 7, 2011 22:32	Sept. 10, 2011 04:40	2.3	1.3 ± 0.1	652	19.9	−64	X1.8	N14W18
3	Sept. 24, 2011 09:21	Sept. 26, 2011 13:50	2.2	0.8 ± 0.1	704	34.2	−103	X1.9	N12E60
4	Jan. 27, 2012 17:37	Jan. 31, 2012 15:20	3.9	1.1 ± 0.1	427	10.8	−19	X1.7	N27W71
5	Mar. 7, 2012 04:00	Mar. 8, 2012 11:20	1.3	2.4 ± 0.2	737	23.1	−145	X5.4	N17E27
6	July 12, 2012 15:37	July 14, 2012 18:30	2.1	1.8 ± 0.2	667	27.3	−133	X1.4	S15W01
7	May 13, 2013 15:48	May 15, 2013 16:30	2.0	1.1 ± 0.1	440	10.8	−57	X2.8	N11E85
8	Oct. 28, 2013 01:41	Oct. 29, 2013 18:40	1.7	0.8 ± 0.1	436	12.1	−50	X1.0	N04W66
9	Sept. 10, 2014 17:21	Sept. 12, 2014 11:20	1.7	1.5 ± 0.1	730	31.7	−75	X1.6	N14E02
10	Nov. 7, 2014 16:53	Nov. 9, 2014 11:10	1.8	0.9 ± 0.1	606	19.4	−57	X1.6	N14E36
11	Dec. 20, 2014 00:11	Dec. 23, 2014 13:10	3.5	1.7 ± 0.1	562	28.7	−38	X1.8	S21W24
12	Sept. 6, 2017 11:53	Sept. 8, 2017 00:50	1.5	2.0 ± 0.2	821	27.3	−142	X9.3	S08W33
13	Sept. 10, 2017 15:35	Sept. 13, 2017 11:40	2.8	1.3 ± 0.2	622	13.7	−50	X8.2	S09W84

ANALYZING FORBUSH DECREASES CAUSED BY POWERFUL X-CLASS SOLAR FLARES

Table 1 presents the time a flare beginning, the start of the FE, difference Δt (days) between the beginning of a flare and the start of the FE, amplitude of the FE in the muon flux A_{FD} (%), speed of the solar wind V_{SW} (km/s), modulus of the vector of magnetic induction B (nT), index of geomagnetic activity Dst_{min} (nT) [6], and the class of the flare and its coordinates. No such events were observed in the periods 2007–2010 and 2018–2019 (during periods of minimum solar activity). The start of the Forbush effect was determined from MH URAGAN data by determining FE characteristics [7]. Using MH URAGAN data for the period 2012–2017, we identified 56 FEs with amplitudes of more than 0.5% and obtained correlations with the parameters of heliospheric and geomagnetic disturbances [8].

Figure 1 gives correlation dependences of amplitude decrease A_{FD} on (a) speed of the solar wind V_{SW} (coefficient of correlation $R = 0.58 \pm 0.04$), (b) mag-

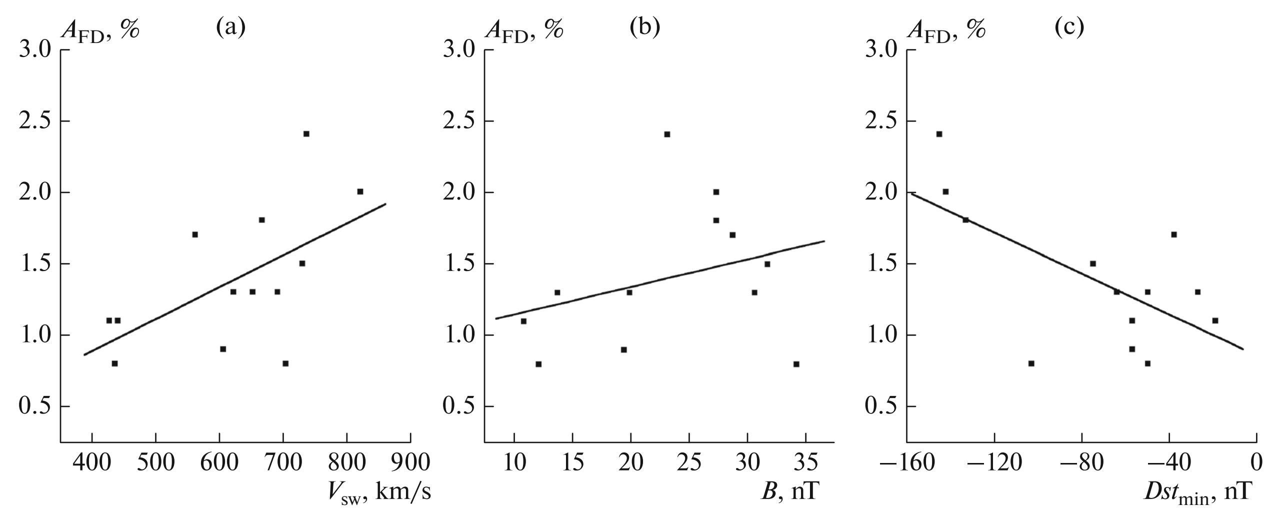

Fig. 1. Correlation dependences of FE amplitude A_{FD} according to MH URAGAN data with (a) solar wind speed V_{sw} (coefficient of correlation $R = 0.58 \pm 0.04$), (b) modulus of the magnetic induction vector B ($R = 0.3 \pm 0.3$), and (c) Dst_{min} index ($R = -0.64 \pm 0.02$) for 13 events caused by X-class flares. The dots represent experimental data, and the line is the linear fit.

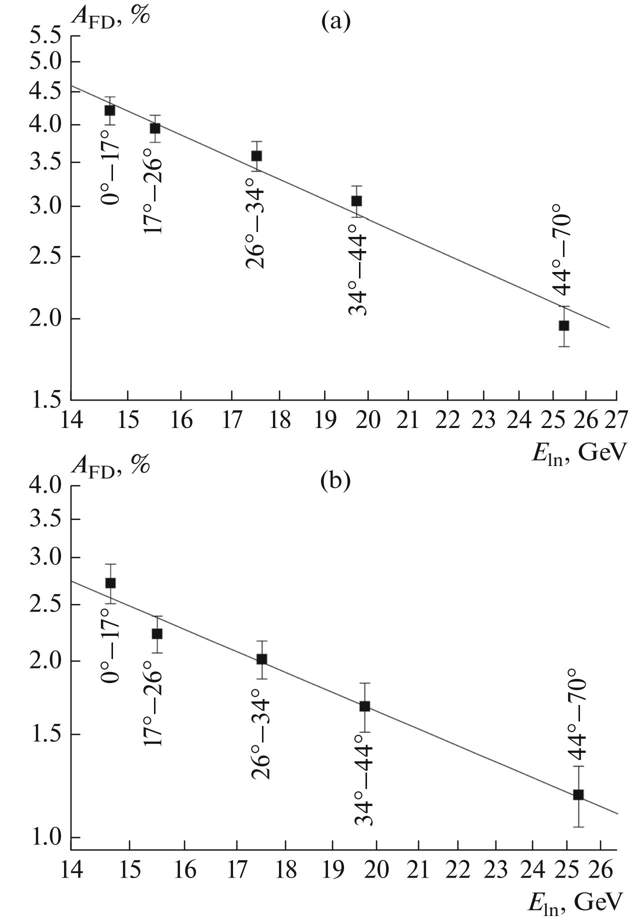

Fig. 2. FE amplitudes of (a) March 8, 2012, and (b) September 8, 2017, as functions of the logarithmic mean energies of primary CRs contributing to the change in the MH URAGAN counting rate for the five zenith angle intervals.

netic induction vector B ($R = 0.3 \pm 0.3$), and (c) index Dst_{min} ($R = -0.64 \pm 0.02$).

Event of March 8, 2012

An X5.4 class flare occurred on March 7, 2012, in NOAA active region (AR) 11429 located in the northeast quadrant of the solar disk. The flare was associated with a very rapid coronal mass ejection (CME) that had a speed of around 2700 km/s. This flare was the second strongest event in the 24th solar cycle, and it caused a G3 level geomagnetic storm.

Amplitude spectrum index α was calculated from the dependence of the amplitudes of the Forbush decrease on the logarithmic mean energies of primary CRs contributing to the change in the counting rate of muon hodoscope during the FEs. The five zenith angle intervals of 0°–17°, 17°–26°, 26°–34°, 34°–44°, and >44° correspond to logarithmic mean energies (E_{ln}) 14.7, 15.5, 17.5, 19.7, and 25.3 GeV. The obtained dependence was fitted with power function E^{α} [9, 10].

It is seen from Fig. 2a that the effect was manifested to a large degree even in the region of high energies (~24 GeV): the reduction in the fifth range of angles was $2.0 \pm 0.1\%$. This indicates that the influence of the heliospheric disturbance on cosmic rays extended at energies above 24 GeV. Amplitude spectrum index α was -1.3 ± 0.2.

Event of September 8, 2017

Flare X9.3/2B occurred on September 6, 2017. Its coordinates were S08 W33, the time of its maximum was 12:02 UT, and its duration was 17 min. The flare was accompanied by a coronal mass ejection (speed 1100–1200 km/s) with a component directed toward the Earth and proton fluxes in a wide range of energies. An accelerated flux from the CME arrived at the start of the day on September 8, 2017. The speed of the solar wind increased sharply to 847 km/s, and fluctuations of the south component of the interplanetary magnetic field were amplified. Figure 2b shows the dependence of the FE amplitudes of September 8, 2017, on the logarithmic mean energies of primary CRs contributing to the change in the MH URAGAN counting rate for the five zenith angle intervals listed above. Amplitude spectrum index α was -1.4 ± 0.2. The reduction in the fifth range of angles was $1.2 \pm 0.1\%$.

CONCLUSIONS

Thirteen FEs caused by powerful X-class solar flares were selected for the period 2007–2019. The FE of March 8, 2012, considered in detail was more powerful than the event of September 8, 2017. The Forbush decreases amplitude in the integral counting rates were $2.4 \pm 0.2\%$ and $2.0 \pm 0.2\%$, respectively. For both events, the influence of the heliospheric disturbance on cosmic rays extended at energies above 24 GeV. The coefficient of correlation between FE amplitudes A_{FD} and solar wind speed V_{sw} was $R = 0.58 \pm 0.04$, with the modulus of magnetic induction vector B, $R = 0.3 \pm 0.3$; with geomagnetic activity index Dst_{min}, $R = -0.64 \pm 0.02$. Results show good correspondence between the parameters of heliospheric and geomagnetic disturbances and FE amplitudes A_{FD}.

ACKNOWLEDGMENTS

This work was performed with data from the Unique Scientific Facility NEVOD.

FUNDING

This work was supported by the Russian Science Foundation, project no. 17-17-01215.

REFERENCES

1. Yasyukevich, Y., Astafyeva, E., Padokhin, A., et al., *Space Weather*, 2018, vol. 16, p. 1013.
2. Forbush, S.E., *J. Geophys. Res.*, 1954, vol. 59, p. 525.
3. Mavromichalaki, H., Papaioannou, A., Plainaki, C., et al., *Adv. Space Res.*, 2011, vol. 47, p. 2210.
4. Rockenbach, M., Dal Lago, A., Schuch, N.J., et al., *Space Sci. Rev.*, 2014, vol. 182, p. 1.
5. Barbashina, N.S., Kokoulin, R.P., Kompaniets, K.G., et al., *Instrum. Exp. Tech.*, 2008, vol. 51, p. 180.
6. Goddard Space Flight Center, Space Physics Data Facility. https://omniweb.gsfc.nasa.gov/ow.html.
7. Barbashina, N.S., Dmitrieva, A.N., Kompaniets, K.G., et al., *Bull. Russ. Acad. Sci.: Phys.*, 2009, vol. 73, no. 3, p. 343.
8. Kovylyaeva, A.A., Astapov, I.I., Barbashina, N.S., et al., *Bull. Russ. Acad. Sci.: Phys.*, 2019, vol. 83, no. 5, p. 563.
9. Yakovleva, E.I., Bogdanov, A.G., Dmitrieva, A.N., et al., *Bull. Russ. Acad. Sci.: Phys.*, 2009, vol. 73, no. 3, p. 357.
10. Barbashina, N.S., Astapov, I.I., Borog, V.V., et al., *J. Phys.: Conf. Ser.*, 2013, vol. 409, 012189.

Translated by A. Nikol'skii